

## Flame Retardant Polyurethane Elastomer Nanocomposite Applied to Coal Mines as Air-Leak Sealant

Jianming Wu,<sup>1</sup> Hong Yan,<sup>2</sup> Junfeng Wang,<sup>1</sup> Yuguo Wu,<sup>1</sup> Chunshan Zhou<sup>1</sup>

<sup>1</sup>College of Mining Technology, Taiyuan University of Technology, Taiyuan, Shanxi 030024, People's Republic of China

<sup>2</sup>College of Materials Science and Engineering, Taiyuan University of Technology, Taiyuan, Shanxi 030024, People's Republic of China

Correspondence to: J. Wu (E-mail: tyutwjm@163.com)

**ABSTRACT:** Polyurethane elastomer (PUE) was firstly applied to mining coal roadway as air-leak sealant. It is very important for air-leak sealants to possess the super mechanical properties and good flame retardant performance when applied to the coal-rock mass with cracks. The reinforced and toughened PUE nanocomposites were obtained by adding surface modified TiO<sub>2</sub> and SiO<sub>2</sub> nanoparticles. The modified PUE was characterized in terms of morphology, structure, and thermal stability by field-emission scanning electron microscopy (FESEM), X-ray diffraction (XRD), infrared spectroscopy (IR), and thermogravimetric analysis (TGA). Its flame-retardant performance and mechanical properties were also tested. The results showed that the surface modified nanoparticles were uniformly dispersed in the PUE matrix and enhanced its thermal stability and flame retardant performance. The dual effects of uniform dispersion of nanoparticles and hydrogen bonding between nanoparticles and PUE improved the mechanical properties of the composites. The PUE modified by nanoparticles was successfully applied to coal mines and showed great air-leak sealing effect.

© 2013 Wiley Periodicals, Inc. *J. Appl. Polym. Sci.* 000: 000–000, 2013

**KEYWORDS:** nanoparticles; mechanical properties; polyurethanes; flame retardance; composites

Received 30 September 2012; accepted 20 December 2012; published online

**DOI:** 10.1002/app.38946

### INTRODUCTION

Polyurethanes (PUs) are an important class of polymers that have wide application in a number of different industrial sectors. Segmented PUs, consisting of hard and soft segments, are known to have microphase separated structure, which makes them to be used in various ways such as adhesives,<sup>1</sup> coatings,<sup>2</sup> biomaterials,<sup>3–5</sup> shape memory material,<sup>6</sup> and actuator.<sup>7–9</sup> Polyurethane elastomers (PUEs) are possibly the most versatile classes of polymers as they can be molded, injected, extruded, and recycled.<sup>10</sup> For advanced PUs materials, PUs can be further improved via incorporation of various fillers, including silicates,<sup>11–14</sup> carbon nanotubes,<sup>15–17</sup> glass,<sup>18</sup> nanofiber,<sup>19</sup> graphene,<sup>20</sup> and nanoparticles.<sup>21–23</sup> However, PUs are easily flammable, so their flammability and flame spread are minimized by using different flame retardant additives based on halogen and halogen-free materials.<sup>24–26</sup> The latter attracts growing interest because they are environmental friendly.

To the best of our knowledge, no research focuses on PUE used as air-leak sealant applied to coal mines. The spontaneous combustion of coal, one of the serious disasters in coal mine, threatens people's personal safety and property seriously, affects the

social stability, and has been hindering the sustainable development of coal industry. Furthermore, air leakage is one of the vital causes for the coal spontaneous combustion. So we address the new application of PUE as air-leak sealant in the coal mines. In view of the flammability of PUE presenting a threat to both the integrity of the product and to the safe production of coal mine, the thermal stability and flame retardancy of PUE were enhanced by the addition of silica and titania nanoparticles in this work.

### EXPERIMENTAL

#### Materials

Nano-silica (mean size = 30 nm) was purchased from Shanxi Tond Chemical Comapany, China. Nano-titania (mean size = 20 nm) was obtained from Zhoushan Mingri Nanomaterials Co., China. The particles were dried at 120°C for 24 h to eliminate the adsorbed species. The silane coupling agent KH-550 (NH<sub>2</sub>(CH<sub>2</sub>)<sub>3</sub>Si(OC<sub>2</sub>H<sub>5</sub>)<sub>3</sub>) and KH-570 (CH<sub>2</sub>=C(CH<sub>3</sub>)COO(CH<sub>2</sub>)<sub>3</sub>Si(OCH<sub>3</sub>)<sub>3</sub>) from Beijing Chemical Reagents Company were used to modify nano-silica and -titania. Polyoxypropylene glycol (PPG, number average molecular weight = 2000) and diethylene glycol (DEG) were supplied by Tianjin No. 3

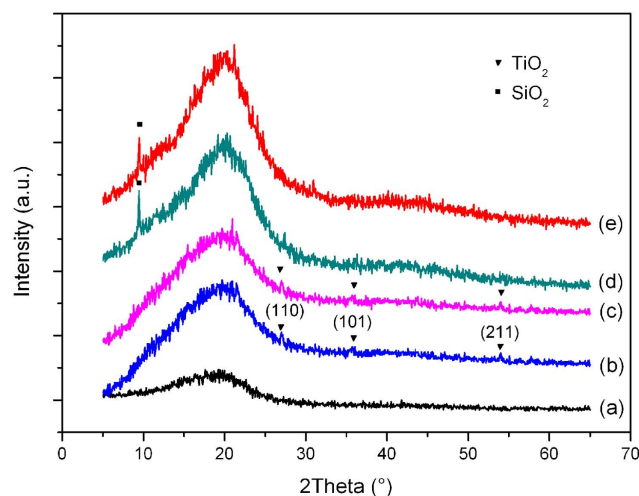


**Figure 1.** XRD patterns of (a) pure PUE, (b) PUE-T1, (c) PUE-T2, (d) PUE-S1, and (e) PUE-S2. [Color figure can be viewed in the online issue, which is available at [wileyonlinelibrary.com](http://wileyonlinelibrary.com).]

Petrochemical Factory, China. Toluene diisocyanate (TDI), methylene-bis-*ortho*-chloroaniline (MOCA, chain extender), and dioctyl phthalate (DOP, plasticizer) were acquired from Shanghai Wulian Chemical Co., China.

#### Surface Modification of Nanoparticles

KH-550 was chosen to modify SiO<sub>2</sub> nanoparticles. A solution with a concentration of 10 wt % was obtained by diluting KH-550 into ethanol, and acetic acid (CH<sub>3</sub>COOH) was dropped into above solution at a constant flow rate until the pH value of 3, under vigorous stirring for 1 h. Then the whole reactive system was heated to 80°C after SiO<sub>2</sub> nanoparticles were added into the mixture solution. After 2 h vigorous stirring, KH-550-modified nano-silica was filtered, washed with deionized water and ethanol for several times, and then dried at 60°C in vacuum.

KH-570 was chosen to modify TiO<sub>2</sub> nanoparticles. Similarly, KH-570-modified nano-titania was obtained according to the above processes.

#### Preparation of PUE Modified by Nanoparticles

About 1 wt % or 2 wt % modified TiO<sub>2</sub> or SiO<sub>2</sub> nanoparticles were added into PPG solution followed by ultrasonic stirring for 30 min. Subsequently, the mixture was transferred into a reactor, and then heated to 110–120°C under a pressure of 0.085–0.09 MPa until the moisture becomes less than 0.05%. After cooling, the mixture was added into TDI solution and the reaction maintained at 80°C for 2 h.

PPG, DEG, MOCA, and DOP were mixed uniformly and then dehydrated for 2–3 h at 110–120°C under a pressure of 0.085–0.09 MPa. The mixture was blended with the resultant obtained from the above procedure for 5–10 min and then cast into a mold. The obtained samples were further characterized and tested. The different samples were named as PUE-T1, PUE-T2, PUE-S1, and PUE-S2.

#### Characterization and Testing

A field-emission scanning electron microscope (FESEM, JSM-6700F, JEOL, Tokyo, Japan) was used to observe the morphologies of PUE nanocomposite samples.

The phase and crystallographic structures of the samples were examined by X-ray diffraction (XRD) on a Y-2000 (Dandong, China) powder diffractometer with CuK $\alpha$  radiation and Ni filter ( $\lambda = 1.54178 \text{ \AA}$ ) at a scan rate of 0.05 °/s.

The thermogravimetric analysis (TGA) was carried out on a TG-209 thermoanalyzer (Netzsch, German), N<sub>2</sub> atmosphere, heating rate 10 °C/min. The curves of weight difference between the experimental and theoretical TG curves are computed as follows<sup>27</sup>:  $M_{\text{PUE}}(T)$ : TG curve of pure PUE,  $M_{\text{exp}}(T)$ : TG curve of the PUE nanocomposite,  $M_{\text{th}}(T)$ : theoretical TG curve computed by linear combination between the TG curves of PUE and nanoparticles:  $M_{\text{th}}(T) = x \cdot M_{\text{PUE}}(T) + y \cdot M_{\text{nano}}(T)$ ,  $x + y = 1$  and  $x, y$  are the mass percentage of PUE and nanoparticles in the composite. Because silica and titania nanoparticles are stable oxides, no weight loss occurs during the TG test.  $M_{\text{nano}}$ , therefore, should be 100 here.  $\Delta(T)$ : curve of weight difference:  $\Delta(T) = M_{\text{exp}}(T) - M_{\text{th}}(T)$ . The  $\Delta(T)$  curves allow the observation of an eventual increase or decrease in the thermal stability of the polymer.

The Fourier transform infrared (FTIR) absorption spectra were recorded on a Bio-Rad (Hercules, CA) FTS-165 spectrometer.

The limiting oxygen index (LOI) values were measured on a HC-2C oxygen index meter (Jiangning Analysis Instrument Company, China) with sheet dimensions of 150 mm  $\times$  10 mm  $\times$  4 mm according to ASTM D2863-97.

## RESULTS AND DISCUSSION

#### XRD Analysis

Figure 1 shows the XRD patterns of different samples. It can be seen that the diffraction peak at  $2\theta$  of 19.32° corresponds to the soft segment of the pure PU,<sup>9</sup> while the characteristic peaks of

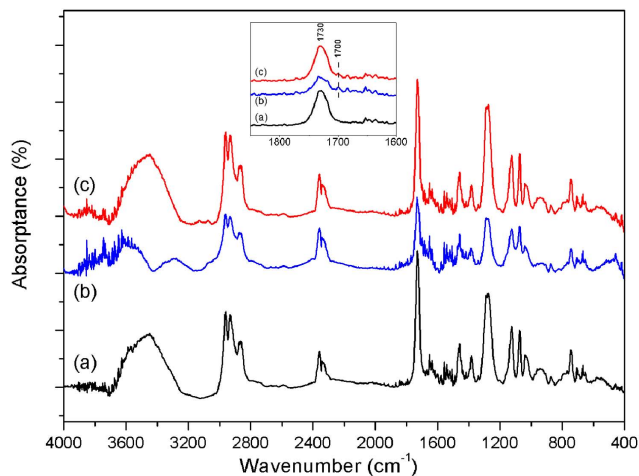


**Figure 2.** Infrared spectra of (a) PUE, (b) PUE-T2, and (c) PUE-S2. [Color figure can be viewed in the online issue, which is available at [wileyonlinelibrary.com](http://wileyonlinelibrary.com).]

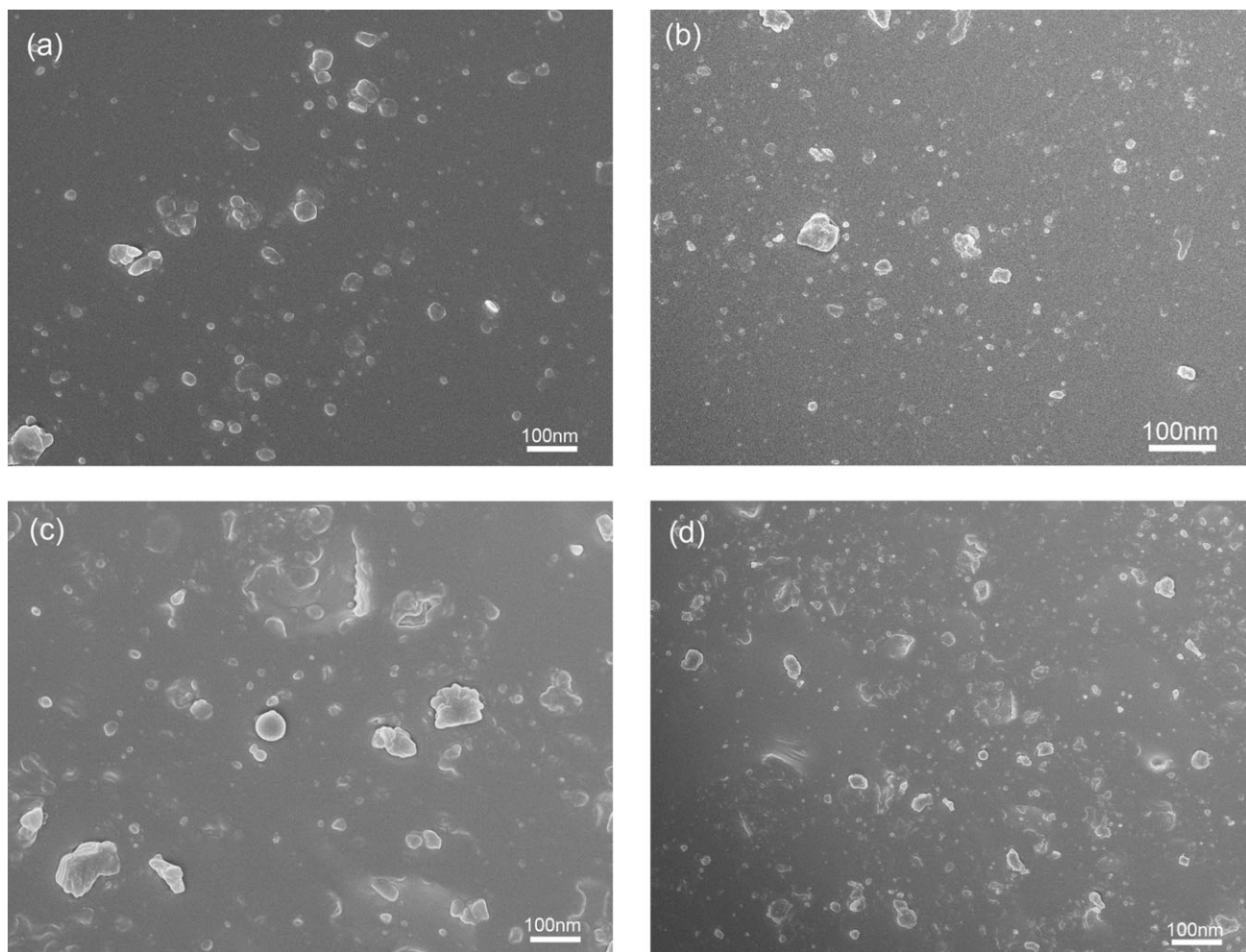


**Figure 3.** FESEM images of surface of different samples (a) PUE-T1, (b) PUE-T2, (c) PUE-S1, (d) PUE-S2.

nanoparticles occur in the composites. The characteristic peaks at  $2\theta$  of approximately  $27^\circ$ ,  $36^\circ$ , and  $54^\circ$  in Figure 1(b,c) could be indexed as the rutile titania with lattice constants comparable to the values of JCPDS 21-1276, corresponding to the crystal

planes of (110), (101), and (211). Moreover, the characteristic peak of silica occurs at  $2\theta$  of approximately  $9.45^\circ$  in Figure 1(d,e).

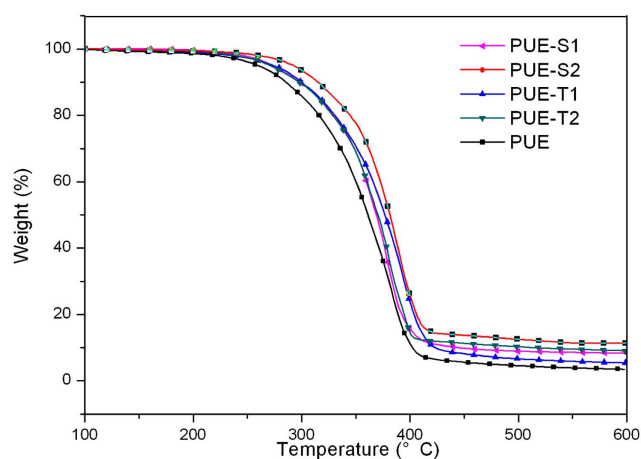


**Figure 4.** TGA curves of different samples. [Color figure can be viewed in the online issue, which is available at [wileyonlinelibrary.com](http://wileyonlinelibrary.com).]

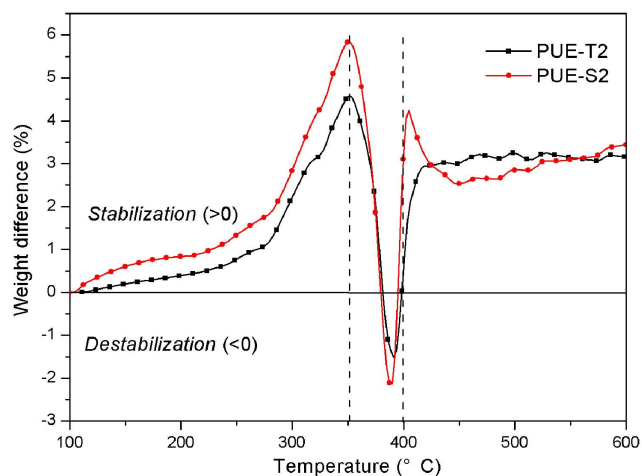


**Figure 5.** Curves of weight difference of experimental and theoretical weight loss of PUE-T2 and -S2. [Color figure can be viewed in the online issue, which is available at [wileyonlinelibrary.com](http://wileyonlinelibrary.com).]

**Table I.** Mechanical properties of different samples

Items	pure PUE	PUE-T1	PUE-T2	PUE-S1	PUE-S2
Shore A Hardness	44	44	46	44	50
Impact elasticity (%)	22	26	32	22	30
Elongation at break (%)	610	820	860	770	830
Tensile strength (MPa)	2.45	3.14	3.47	3.12	3.21
Permanent deformation at break (%)	10	12	16	12	15
Tearing strength (KNm <sup>-1</sup> )	15.2	18.11	20.13	16.94	18.88

**Table II.** LOI values of different samples

Sample ID	Pure PUE	PUE-T1	PUE-T2	PUE-S1	PUE-S2
LOI/%	19	22	23	22.5	25

### FTIR Analysis

Figure 2 shows the FTIR absorption spectra for the samples of PUE, PUE-T2, and -S2. The multiple peaks at 2850–2970 cm<sup>-1</sup> correspond to stretching mode of C—H in CH<sub>2</sub> and CH<sub>3</sub>.<sup>28</sup> The absorption region at 1680–1750 cm<sup>-1</sup> is assigned to carbonyl stretching vibrations in PUE. The sharp and intense peak at 1730 cm<sup>-1</sup> can be attributed to the free C=O stretching vibration of PUE, while the weak peaks at 1700 cm<sup>-1</sup> in Figure 2(b,c) correspond to hydrogen-bonded carbonyl groups,<sup>29–31</sup> indicating the interaction between nanoparticles and PUE in hydrogen bonding.

### SEM Analysis

Figure 3 shows FESEM images of surface of different samples. The white particles in Figure 3(a–d) are nanoparticles with nearly spherical shape, which are uniformly dispersed in the PUE matrix. No obvious gap observed from the images indicates good compatibility between modified nanoparticles and the matrix. Compared with silica nanoparticles, titania nanoparticles shows better dispersibility due to few larger aggregates observed.

### Thermogravimetric Analysis

TGA curves were determined to investigate the thermal stability of different samples, as shown in Figure 4. It can be seen that only one stage of weight loss for different samples and the addition of nanoparticles could enhance their initial degradation temperature to a varied extent. The pure PUE starts to degrade at 274°C, before PUE-S1, PUE-T1, and PUE-T2 which nearly degrade at about 277°C. But the initial and final degradation temperatures for PUE-S2 were enhanced to 292°C and 420°C, respectively. The residual weights for different samples are 1.1% (PUE), 3.04% (PUE-T1), 6.63% (PUE-T2), 5.81% (PUE-S1), and 8.32% (PUE-S2), respectively, indicating that nanoparticles are in favor of the charring formation of PUE. To investigate the interactions between nanoparticles and PU during degradation, the curves of weight difference is plotted (Figure 5). It is shown that interactions are observed (chaotic behavior between stabilization and destabilization of the polymer) between 350 and nearly 400°C. They can be assigned to the fast degradation of PUE and the restriction of mobility of PUE chains by nano-

particles is weakened. Below 350°C and after 400°C, an obvious stabilization of the polymer is observed. It follows that silica and titania nanoparticles could improve the thermal stability of PUE, especially with the addition of 2% of silica.



**Figure 6.** Photographs of PUE in operation with flexible thickness (a) thin coating and (b) thick coating. [Color figure can be viewed in the online issue, which is available at [wileyonlinelibrary.com](http://wileyonlinelibrary.com).]



**Figure 7.** Photograph of modified PUE applied to coal mine. [Color figure can be viewed in the online issue, which is available at [wileyonlinelibrary.com](http://wileyonlinelibrary.com).]

It was reported that if silica nanoparticles uniformly disperse in the polymer matrix, the interfacial area between nanoparticles and matrix would increase by an order of magnitude or more and the thermal stability of composite would be improved,<sup>32</sup> due to the formation of tightly bound polymer chains (bounded polymer chains and their mobility is restricted) around silica particles.<sup>33</sup> Titania nanoparticles have the similar effects on the improvement of the stability of PUE.

#### Mechanical Properties of Modified PUE Composites

Hardness values of the samples were measured according to ASTM D2240 and all the results of mechanical properties are listed in Table I. Shore A hardness has increasing trend with the addition of nanoparticles, and silica shows greater enhancement of hardness at the same addition of 2%, due to its 3D network crystal structure. For the other mechanical properties, however, titania plays a major role than silica, possibly caused by the better dispersion of titania nanoparticles in the matrix.

The interfacial interaction between nanoparticles and matrix (hydrogen bonding) and the uniform dispersion are the key to the enhancement of mechanical properties of PUE. Owing to the huge specific surface area of nanoparticles, the contact areas between fillers and matrix increase greatly. On one hand, the high modulus inorganic rigid nanoparticles enhance the whole modulus of composites and the stress dispersion. On the other hand, the stress concentration caused by nanoparticles under external force leads to shear yield of the composite, which is in favor of the improvement of toughness.

#### LOI Test and Flame Retardant Mechanism

The figures of LOI for different samples are listed in Table II. The LOI value for pure PUE is only 19%, indicating that pure PUE is flammable. The LOI values of composites rise with the increase of nanoparticles' loading. For the same loading, 2 wt % of silica could give an obvious improvement on flame retardant performance of PUE than titania.

Silica or titania nanoparticles having a large surface area and low density significantly increased the polymer melt viscosity of PUE during its gasification or burning. Consequently, the additives accumulated near the sample surface without sinking through the polymer melt layer. The accumulated silica or titania acted as an insulation layer and possibly as a barrier to the transport of degradation products to the surface. Furthermore, the accumulated silica or titania reduced the concentration of PUE near the surface. These layers acted not only as thermal insulation to protect virgin polymer, but also acted as barriers against the migration of the thermal degradation products to the surface.<sup>33</sup> It is noted that silicon is an effective flame retardant element relative to titanium, so silica shows better flame retardant performance.

#### Application to Coal Mine as Air-Leak Sealant

PUE modified by nanoparticles has been applied to some coal mines as air-leak sealant, which is flexible for the coating operation. Figure 6(a) shows the thin coating effect, suitable for the coal seams with small cracks, and Figure 6(b) shows the thick coating, suitable for the coal seams with large cracks. After solidification, modified PUE would deform with the deformation of the coal-rock mass, without cracks and difficult to fall off, as shown in Figure 7. The air leakage rate reduced by 90%, achieving a great sealing effect in the air-leak area.

#### CONCLUSIONS

Due to high elasticity and strength and good adhesion, PUE was chosen as air-leak sealant for coal mines and modified by silica and titania nanoparticles to enhance its flame retardant performance and mechanical properties. After surface modification by silane coupling agent, silica and titania nanoparticles uniformly dispersed in the PUE matrix with good compatibility. With the addition of 2 wt % of silica nanoparticles, the thermal decomposition temperature of PUE composite was enhanced by 20°C. Silica and titania nanoparticles are favorable to the improvement of flame retardant performance of PUE. The values of LOI of composites are 23% and 25%, respectively, with 2 wt % of TiO<sub>2</sub> and SiO<sub>2</sub>, ensuring the safe use of PUE as air-leak sealant in the coal mines. It follows that silica shows the better flame retardancy for PUE than titania.

#### ACKNOWLEDGMENTS

This work was financially supported by International Scientific and Technological Cooperation Project from the Ministry of Science and Technology of China (No. 2010DFB90690), National Natural Science Foundation of China (No. 51274146) and Science and Technology Foundation of Shanxi Province (No. 20120321006).

#### REFERENCES

1. Tyczkowski, J.; Krawczyk-Kłys, I.; Kuberski, S.; Makowski, P. *Eur. Polym. J.* **2010**, *46*, 767.
2. Golaz, B.; Michaud, V.; Manson, J. A. E., *Int. J. Adhes. Adhes.* **2011**, *31*, 805.
3. Merlin, D. L.; Sivasankar, B. *Eur. Polym. J.* **2009**, *45*, 165.

4. Puskas, J.; Elfray, M.; Tomkins, M.; Dossantos, L.; Fischer, F.; Altstadt, V. *Polymer* **2009**, *50*, 245.
5. Zia, K. M.; Zuber, M.; Bhatti, I. A.; Barikani, M.; Sheikh, M. A. *Int. J. Biol. Macromol.* **2009**, *44*, 18.
6. Zia, K. M.; Zuber, M.; Barikani, M.; Bhatti, I. A.; Khan, M. B. *Colloid Surf B* **2009**, *72*, 248.
7. Ask, A.; Menzel, A.; Ristinmaa, M. *Mech. Mater.* **2012**, *50*, 9.
8. Petit, L.; Guiffard, B.; Seveyrat, L.; Guyomar, D. *Sensor Actuat. A Phys.* **2008**, *148*, 105.
9. Raja, M.; Shanmugaraj, A. M.; Ryu, S. H.; Subha, J. *Mater. Chem. Phys.* **2011**, *129*, 925.
10. Zia, K. M.; Barikani, M.; Zuber, M.; Bhatti, I. A.; Barmar, M. *Int. J. Biol. Macromol.* **2009**, *44*, 182.
11. An, L.; Pan, Y. Z.; Shen, X. W.; Lu, H. B.; Yang, Y. L. *J. Mater. Chem.* **2008**, *18*, 4928.
12. Chen, B.; Evans, J. R. G.; Greenwell, H. C.; Boulet, P.; Covey, P. V.; Bowden, A. A.; Whiting, A. *Chem. Soc. Rev.* **2008**, *37*, 568.
13. Wang, C.; Wang, Y.; Liu, W.; Yin, H.; Yuan, Z.; Wang, Q.; Xie, H.; Cheng, R. *Mater. Lett.* **2012**, *78*, 85.
14. Chen, H. X.; Lu, H. Z.; Zhou, Y.; Zheng, M. S.; Ke, C. M.; Zeng, D. L. *Polym. Degrad. Stab.* **2012**, *97*, 242.
15. Wang, C. S.; Chen, X. Y.; Xie, H. F.; Cheng, R. S. *Compos. A* **2011**, *42*, 1620.
16. Xie, H.; Liu, B.; Yuan, Z.; Shen, J.; Cheng, R. *J. Polym. Sci. Part B: Polym. Phys.* **2004**, *42*, 3701.
17. Xiong, J.; Zheng, Z.; Song, W.; Zhou, D.; Wang, X. *Compos. A* **2008**, *39*, 904.
18. Husic, S. *Compos. Sci. Technol.* **2005**, *65*, 19.
19. Barick, A. K.; Tripathy, D. K. *Compos. A* **2010**, *41*, 1471.
20. Cai, D. Y.; Yusoh, K.; Song, M. *Nanotechnology* **2009**, *20*, 085712.
21. Li, J. H.; Hong, R. Y.; Li, M. Y.; Li, H. Z.; Zheng, Y.; Ding, J. *Prog. Org. Coat.* **2009**, *64*, 504.
22. Sheikh, F. A.; Kanjwal, M. A.; Saran, S.; Chung, W. J.; Kim, H. *Appl. Surf. Sci.* **2011**, *257*, 3020.
23. Chen, X. D.; Wang, Z.; Liao, Z. F.; Mai, Y. L.; Zhang, M. Q. *Polym. Test.* **2007**, *26*, 202.
24. Huang, G.; Gao, J.; Li, Y.; Han, L.; Wang, X. *Polym. Degrad. Stab.* **2010**, *95*, 245.
25. Thirumal, M.; Khastgir, D.; Nando, G. B.; Naik, Y. P.; Singha, N. K. *Polym. Degrad. Stab.* **2010**, *95*, 1138.
26. Tirri, T.; Aubert, M.; Wilén, C.-E.; Pfaendner, R.; Hoppe, H. *Polym. Degrad. Stab.* **2012**, *97*, 375.
27. Lewicki, J. P.; Pielichowski, K.; De La Croix, P. T.; Janowski, B.; Todd, D.; Liggat, J. J. *Polym. Degrad. Stab.* **2010**, *95*, 1099.
28. Chen J.; Rong M.; Ruan W.; Zhang M. *Compos. Sci. Technol.* **2009**, *69*, 252.
29. Zhang, J.; Hu, C. P. *Eur. Polym. J.* **2008**, *44*, 3708.
30. Amrollahi, M.; Sadeghi, G. M. M.; Kashcooli, Y. *Mater. Design* **2011**, *32*, 3933.
31. Pei, A.; Malho, J.-M.; Ruokolainen, J.; Zhou, Q.; Berglund, L. A. *Macromolecules* **2011**, *44*, 4422.
32. Kashiwagi, T.; Shields, J. R.; Harris, R. H.; Davis, R. D. *J. Appl. Polym. Sci.* **2003**, *87*, 1541.
33. Kashiwagi, T.; Gilman, J. M.; Butler, K. M.; Harris, R. H.; Shields, J. R.; Asano, A. *Fire Mater* **2000**, *24*, 277.